Build-up and decline of organic matter during PeECE III

K. G. Schulz, U. Riebesell, R. G. J. Bellerby, H. Biswas, M. Meyerhöfer, M. N. Müller, J. K. Egge, J. C. Nejstgaard, C. Neill, J. Wohlers, et al.

Biogeosciences Discuss., 4, 4539–4570, 2007
www.biogeosciences-discuss.net/4/4539/2007/

Biogeosciences Discussions

Biogeosciences Discussions is the access reviewed discussion forum of *Biogeosciences*

Build-up and decline of organic matter during PeECE III

K. G. Schulz[1], U. Riebesell[1], R. G. J. Bellerby[2,3], H. Biswas[1], M. Meyerhöfer[1], M. N. Müller[1], J. K. Egge[4], J. C. Nejstgaard[4], C. Neill[2], J. Wohlers[1], and E. Zöllner[1]

[1]Leibniz Institute for Marine Sciences (IFM-GEOMAR), Düsternbrooker Weg 20, 24105 Kiel, Germany
[2]Bjerknes Centre for Climate Research, Univ. of Bergen, Allégaten 55, 5007 Bergen, Norway
[3]Geophysical Institute, Univ. of Bergen, Allégaten 70, 5007 Bergen, Norway
[4]University of Bergen, Department of Biology, Box 7800, 5020 Bergen, Norway

Received: 13 November 2007 – Accepted: 13 November 2007 – Published: 30 November 2007

Correspondence to: K. Schulz (kschulz@ifm-geomar.de)

Abstract

Increasing atmospheric carbon dioxide (CO_2) concentrations due to anthropogenic fossil fuel combustion currently change the ocean's chemistry. Increasing oceanic [CO_2] and subsequent decreasing seawater pH have the potential to significantly impact marine life. Here we describe and analyze the build-up and decline of a natural phytoplankton bloom initiated during the 2005 mesocosm Pelagic Ecosystem CO_2 Enrichment study (PeECE III). We show that processes of inorganic carbon uptake in mixed surface waters and organic carbon export to depth were significantly enhanced at elevated CO_2, while ammonium regeneration in deep waters was substantially reduced. This has important implications for our understanding of pelagic ecosystem functioning and future carbon cycling.

1 Introduction

Human activities such as the massive combustion of fossil fuels perturb the natural carbon cycle by increasing atmospheric carbon dioxide [CO_2] concentrations. Since the beginning of the industrial revolution atmospheric CO_2 levels have increased already from about 280 to 380 μatm, in the year 2006 and are projected to reach values as high as 700 μatm, by the end of the 21. century (IPCC, 2001). Together with changes in other climate relevant gases this substantial increase in atmospheric CO_2 drives global climate change: increasing global mean temperatures, rising sea level and accelerating extreme weather incidences, to name just those events most likely to happen (IPCC, 2007). As a result of atmosphere-ocean gas exchange increasing atmospheric CO_2 levels are accompanied by concomitant increases of [CO_2] in ocean surface waters. This leads to a redistribution in the oceanic dissolved inorganic carbon (DIC) pool, resulting in increased ocean acidity on one hand and reduced carbonate saturation state on the other. This is manifested in decreasing ocean pH which is very likely do drop about 0.4 units until the end of the 21. century, adding to the 0.1 unit drop

BGD

4, 4539–4570, 2007

already observed since the beginning of the industrial revolution (Caldeira and Wicket, 2003).

Most of the marine organisms studied so far are known to be sensitive in some way or the other to changes in ocean chemistry (for a review see Riebesell (2005)). Marine biogenic calcification ($CaCO_3$ formation), for instance, by warm water corals, coccolithophores and foraminifera has been shown to decrease with increasing pH and hence decreasing carbonate saturation (Gattuso et al., 1998; Kleypas et al., 1999; Riebesell et al., 2000; Russel et al., 2004). Although the response of biogenic $CaCO_3$ production to changing ocean chemistry may differ between species (Langer et al., 2006) and is far from being understood, if carbonate saturation drops below unity the calcareous shells of these organisms begin to dissolve. This will probably happen towards the end of the 21. century to another important group of pelagic calfifiers, the pteropods. Their natural habitats, the Southern Ocean and the subarctic Pacific, will become undersaturated with respect to their $CaCO_3$ (aragonite) shells at increasing CO_2 levels (Orr et al., 2005). Marine phytoplankton has also been shown to change their elemental composition (C/N/P) in response to changing [CO_2] (Burkhardt and Riebesell, 1997; Burkhardt et al., 1999b). But again, these changes were species-specific, sometimes even with opposite sign. Furthermore, increases in C/N can be the result of increased production of transparent exopolymer particles, TEP, (Engel , 2002) which are believed to be important for the export of particulate organic matter from the sunlit surface ocean to its interior (Engel et al., 2004). Whether carbon and nitrogen remineralization rates at depth could be effected by varying C/N is another open question. Thus, increasing atmospheric and surface ocean CO_2 levels have the potential to change marine element cycling which could trigger important feedback responses in Earth's climate system.

While laboratory studies provide process based understanding at the organismal level mesocosms are ideal for perturbation experiments at the community level. However, a solid experimental design and setup are crucial for subsequent data interpretation. Here we describe the mesocosm setup and performance as well as the temporal

development of the phytoplankton bloom in terms of build-up of particulate and dissolved organic matter and changes in respective carbon to nitrogen to phosphorus ratios for the 2005 Pelagic Ecosystem CO_2 Enrichment study (PeECE III).

2 Methods

2.1 Mesocosm setup and sampling

In May 2005, in the Raunefjorden at the coastline of Norway (~60°16′′ N, 5°13′′ E) nine polyethylene bags (see Fig. 1 for a graphical representation), 2 m in diameter and extending about 9.5 m into depth, were deployed at a free floating raft, operated by the University of Bergen. The bags were filled simultaneously with unfiltered nutrient-poor fjord water, about 27 m^3 each, pumped from 13.5 m depth. Three different CO_2 levels ~350 (mesocosms M1–M3), 700 (mesocosms M4–M6) and 1050 μatm (mesocosms M7–M9), termed hereafter 1x, 2x and 3x CO_2, representing present day CO_2 conditions and those predicted for the year 2100 and 2150, respectively (IPCC, 2001), were set up in triplicate following in principle the approach described in Engel et al. (2005).

Briefly, the enclosed fjord water was aerated at target CO_2 levels for about two days until equilibration was reached. Then, about 0.8 m^3 of freshwater were mixed into the upper 5.5 m by aquarium water pumps (flow rate ~450 l h^{-1}), creating a halocline with a salinity gradient of ~1.5 psu at about 5.7 m depth (see Fig. 1). The location and stability of the halocline, separating upper mixed surface from deep waters, was monitored daily by means of a CTD (SAIV A/S, model SD204), providing combined vertical distributions of salinity and temperature within the mesocosms (see Figs. 2 and 3, respectively). The operation of the aquarium water pumps within the upper surface waters throughout the experiment ensured the homogeneous distribution of dissolved compounds. The mesocosm bags were covered with gas tight tents (ETFE foil) which allowed for the transmission of about 95% of the complete sunlight spectrum. Incident PAR, photosynthetic active radiation between 400 and 700 nm, was measured contin-

uously (15 min averages) with a Licor light sensor (LI-190) connected to a datalogger (LI-1400) mounted on the raft (see Fig. 4). On some days this photon flux density (PFD) was also measured within the headspace and at 2.5 m depth of mesocosm M8. The headspace within the tents was continuously flushed with air at target CO_2 values throughout the experiment, simulating a 1x, 2x and 3x CO_2 atmosphere.

The phytoplankton bloom was initiated on day t_{-1} by additions of nitrate and phosphate to upper surface waters aiming for final surface water concentrations of 16 and 0.8 μmol kg^{-1}, respectively (see Fig. 5a, b). However, in mesocosms 1,2,3 and 4 these concentrations were lower than expected as some of the nutrients added must have been lost to deep waters during mixing. Therefore, additional nitrate and phosphate was added to these mesocosms on day t_1, establishing uniform nutrient concentrations within all mesocosms on day 2 (see Fig. 5). As pCO_2 in mesocosms 1–6 were below intended values, $NaHCO_3$ and equimolar amounts of HCl were added, reaching final concentrations of ~25 and ~18 μmol kg^{-1} in mesocosms 1–3 and 4–6, respectively. Regarding the changes in the CO_2 system this procedure is equivalent to CO_2 aeration and increased pCO_2 in mesocosms 1–6 to desired values of ~700 and ~1050 μatm on day 2 (see Fig. 6).

Daily sampling was at 10:00 a.m. starting on day t_0. Dissolved and particulate components (with the exception of DIC, alkalinity, pCO_2, and other gases) were sampled with a 5 m long, 6 cm diameter tube lowered into the mesocosms, providing a depth-integrated sample. The samples representative for upper surface waters (~20 L per mesocosm per day) were brought back to shore where sub-samples for various measurements and analyzes were taken immediately upon arrival. Every other day water from sediment traps, 60×10 cm Plexiglas cylinders deployed in each mesocosm at 7.5 m depth, was also collected.

2.2 Measurements and analyzes

In principle all measurements and analyzes of parameters presented in this article followed standard procedures. A complete list of all parameters measured together with

their individual methods is given in Table 1. For details on measurement methods of parameters not presented in this article the reader is referred to the respective reference given in Table 1.

The nutrients nitrate, nitrite and phosphate were determined from GF/F filtered, silicate from 3 μm cellulose acetate filtered sample water and measured with an autoanalyzer (AA II) according to Hansen and Koroleff (1999). Ammonium was determined following the approach described in Holmes et al. (1999).

For phytoplankton pigment analysis 250–500 ml of sample water were filtered onto GF/F filters which were frozen at −20°C until extraction and analysis. For extraction filters were homogenized together with 2 and 4 mm glass beads in 2 ml 100% acetone by a cooled Vibrogen cell mill for 5 min. Then the samples were centrifuged at ~3000 x g and −10°C for 10 min. The supernatant was 0.2 μm filtered and analyzed by rp-HPLC (reverse-phase high performance liquid chromatography) where pigments are identified by comparing retention times and absorption spectra, obtained with a diode array spectrophotometer (WATERS), with those of pigment standards. Commercially available pigments were also used as standards for calibration. All sample handling during the extraction and analysis procedures were carried out under dimmed light conditions to prevent pigment photo-oxidation. Calculation of the phytoplankton community composition and individual phytoplankton Chl*a* contributions (see Fig. 7) was carried out with the program CHEMTAX (Mackey et al., 1996).

For determination of the particulate compounds TPC (total particulate carbon), POC (particulate organic carbon), PIC (particulate inorganic carbon), PON (particulate organic nitrogen), POP (particulate organic phosphorus) 250–500 ml of sample water were filtered onto precombusted (450°C for 5 h) GF/F filters and stored at −20°C. TPC, POC, and PON were determined on an EuroVector elemental analyzer (EuroEA 3000). Before analysis all filters were dried for 6 h at 60°C, while POC filters had been fumed overnight with concentrated HCl to remove PIC. Particulate inorganic carbon was then calculated as the difference between TPC and POC (see Fig. 8). POP was oxidized by potassium persulphate to dissolved inorganic phosphorus which was measured as

described by Hansen and Koroleff (1999). Every other day these measurements were also performed on 200–250 ml sub-samples collected from all nine sediment traps.

Determination of the dissolved compounds DOC (dissolved organic carbon), DON (dissolved organic nitrogen) and DOP (dissolved organic phosphorus) was on GF/F filtered fjord water samples. DOC and DON were analyzed by means of high temperature catalytic oxidation (HTCO) as described in Qian and Mopper (1996), DOP by potassium persulphate oxidation and subsequent dissolved inorganic phosphorus determination described in Hansen and Koroleff (1999) (see Fig. 8).

3 Results

3.1 Mesocosm performance

Unlike in a previous mesocosm CO_2 perturbation experiment (Engel et al., 2005), deep water was separated from the upper mixed surface by establishing a halocline. This allowed particulate organic matter produced in the nutrient-enriched surface waters to settle into depth, simulating export production. Detailed monitoring of the location and stability of the halocline showed that until day t_{12} deep water loss (mixing of deep waters into the surface waters and deepening of the halocline) was only moderate (~8–21%) in most mesocosms, with the exception of mesocosm M6 (~36%). Unusually stormy weather conditions around day t_{12}, however, enhanced deep water mixing, and until the end of the experiment a substantial portion of the deep water was lost in all mesocosms (~29–42%) with up to 58% and 50% in mesocosms M3 and M6, respectively (Fig. 2).

Temperatures within the mesocosms, initially evenly distributed throughout depth at about 9°C, increased to ~11.5°C in upper surface and ~11°C in deep waters until day t_{19} (Fig. 3). Towards the end of the experiment on day t_{25} temperatures were again distributed homogeneously, although slightly decreased, at about 10.5°C.

Daily averaged incident photon flux densities measured on the raft varied between

90 and 560 μmol m^{-2} s^{-1}. These fluctuations corresponded well with those measured in solar radiation at the University of Bergen (Fig. 4). About 80% of incident PAR passed through the gas tight tents into the mesocosms' headspace of which up to 15% penetrated into ~2.5 m depth, the center of the mixed surface layer (data not shown).

Having established desired pCO_2 values within the mesocosms' surface waters of ~350, 700 and 1050 μatm at day t_2, CO_2 partial pressure continuously decreased until day t_{12} to ~200, 350 and 460 μatm in the 1x, 2x and 3x mesocosms, respectively. After a slight increase on day t_{13} and t_{14} pCO_2 remained rather constant until the end of the experiment (Fig. 6).

All sediment traps, sampled every other day, showed significant over-trapping. In other words more particulate material was calculated to be exported into the deep than inorganic nutrients removed from surface waters. This was probably caused by continuous flapping of the mesocosm bags mainly forced by wind stress which extended into depth and resuspension of sedimented particulate matter. Hence, rather than absolute concentrations only element ratios (POC/PON, POC/POP and PON/POP) are reported in this study (Fig. 11).

3.2 Inorganic nutrient uptake and organic material build-up

Following the addition of nitrate and phosphate on day t_{-1} and their adjustment on day t_1 to 15 and 0.7 μmol kg^{-1} in all mesocosms, respectively, inorganic nutrients (nitrate, phosphate and silicate) continuously decreased (Fig. 5). In all mesocosms silicate was the first to get depleted about day t_7 (Fig. 5c), followed by phosphate about day t_{10} (Fig. 5b) and nitrate about day t_{13} (Fig. 5a). From their day of depletion onwards all inorganic nutrient concentrations remained comparatively low. An exception were ammonium concentrations which were close to zero until day t_{12} and increased up to ~0.5, 0.75 and 0.9 μmol kg^{-1} until day t_{20} in the 1x, 2x and 3x CO_2 mesocosms, respectively (Fig. 5d). Corresponding deep water values also increased to up to 3 μmol kg^{-1} towards the end of the experiment, with apparently higher values in 3x than in 2x and 2x

BGD
4, 4539–4570, 2007

than 1x CO_2 mesocosms (Fig. 5e).

The draw-down in inorganic nutrients was reflected by a concomitant build-up of organic matter. Total Chl*a* concentrations increased from about 1.5 $\mu g\,l^{-1}$ on day t_0 to ~11.0, 13.5 and 13.0 $\mu g\,l^{-1}$ on day t_{10} in the 1x, 2x and 3x CO_2 mesocosms, respectively (Fig. 7a). From then on Chl*a* continuously decreased in all mesocosms, reaching again starting concentrations around day t_{16}. Separating total Chl*a* concentrations into individual contributions by selected phytoplankton taxa showed that diatoms (mostly *Skeletonema* sp. and *Nitzschia* sp.) and prymnesiophytes (including *Emiliania huxleyi*) were of major importance, both reaching up to ~5 $\mu g\,l^{-1}$ in all mesocosms. However, diatom associated Chl*a* peaked about day t_9 while that of prymnesiophytes coincided with the total Chl*a* maximum on day t_{10} (Fig. 7b, c). During and after the decline of the phytoplankton bloom, from day t_{10} onwards, prasinophyte, cyanobacteria and dinoflagellate Chl*a* concentrations were slightly increasing in all mesocosms (Fig. 7d, e, f).

The build-up of particulate organic carbon, nitrogen and phosphorus was very similar to that of Chl*a* with maximum values reached between days t_{10}–t_{12}. However POC, PON and POP concentrations did not decrease to starting values after the decline of the bloom. During the first 10 to 12 days, until the peak of the bloom, about 60–65 $\mu mol\,l^{-1}$ of POC, 9–10 $\mu mol\,l^{-1}$ of PON and 0.4 $\mu mol\,l^{-1}$ of POP accumulated in the upper 5.7 m of all mesocosms of which about 30–35 $\mu mol\,l^{-1}$ of POC, 3.5–4.5 $\mu mol\,l^{-1}$ of PON and 0.15 $\mu mol\,l^{-1}$ of POP remained until the end of the experiment (Fig. 8a, b, c). Due to $CaCO_3$ production of coccolithophores during the phytoplankton bloom (compare Fig. 8c), also about 15 $\mu mol\,l^{-1}$ of PIC was built-up until the peak of the bloom, however almost all $CaCO_3$ produced was lost from the upper mixed layer towards the end of the experiment (Fig. 8d). On the other hand, concentrations of all dissolved organic compounds increased steadily from day t_0 to day t_{24} in all mesocosms, DOC from about 75 to 100 $\mu mol\,l^{-1}$, DON from about 2.5 to 9.5 $\mu mol\,l^{-1}$ and DOP from about 0.2 to 0.25 $\mu mol\,l^{-1}$ (Fig. 8e, f, g).

Finally, in all mesocosms metazooplankton biomass increased from an average

of about 0.7 μmol carbon per liter at the beginning of the experiment to about 3.1–3.5 μmol l^{-1} towards the end (Fig. 9).

3.3 Element ratios of particulate and dissolved organic matter

Individual build-up and removal of both, particulate and dissolved organic matter in the mixed surface waters lead to specific temporal variations in the respective element ratios. The ratio of carbon to nitrogen to phosphorus of particulate matter accumulating in the upper 5.7 m of all mesocosms was close to Redfield with 106/16/1 (POC/PON/POP) until about day t_9. From then on only POC/PON remained close to 6.625 while POC/POP and PON/POP increased about 2-fold to values of ~200 and 30, respectively (Fig. 10a, b, c). This can be the result of preferential POP removal from the upper surface waters. The individual element ratios of the dissolved organic matter build-up during the experiment, however, did not seem to change with time but significantly deviated from Redfield in all mesocosms. DOC/DON was relatively low with about 3, while DOC/DOP and DON/DOP were relatively high with values around 300 and 100, respectively (Fig. 10d, e, f). About 2x lower DOC/DON, 3x higher DOC/DOP and 5x higher DON/DOP in comparison to the corresponding Redfield ratios can be the result of either relatively higher DOP than DOC than DON removal or relatively lower DOP than DOC than DON build-up within the upper surface waters.

The ratios of carbon to nitrogen to phosphorus of the particulate organic material collected in the sediment traps reflect processes of accumulation and remineralization. In all mesocosms sedimentary POC/PON was close to Redfield ratios throughout the experiment (Fig. 11) as were the corresponding values in the upper surface waters (compare Fig. 10a, b, c). Sedimentary POC/POP and PON/POP increased after about 14 days to higher ratios, however, apparently higher in the 3x than 2x than 1x CO_2 mesocosms.

4 Discussion

4.1 Mesocosm performance

The 2005 PeECE III mesocosm experiment differs in several aspects but one substantial from many previous studies, the establishment of a halocline. This was thought to create two distinct water masses in which pelagic key processes such as primary production (surface waters) and remineralization (deep waters) are separated. Any water exchange between these two realms can make data interpretation difficult as most efforts were directed towards sampling in the upper surface waters. Hence, the stability and location of the halocline was monitored on a daily basis. However, even without the storm event on day t_{12}, substantial deep water mixing into the upper surface would have occured. This could have been caused by wind force acting on the mesocosm bags being transmitted into depth. This would also explain the observed over-trapping of the sediment traps caused by significant resuspension of settled particulate organic matter. Complete element budgets and process assessment of primary production and remineralization therefore require sampling in both water masses. Sedimentation processes on the other hand appear to be difficult to evaluate with this kind of mesocosm setup.

4.2 Inorganic nutrient uptake and organic material build-up

The draw-down of the major nutrients nitrate, phosphate and silicate during the bloom phase of the experiment followed the same temporal pattern in all mesocosms, irrespective of pCO_2 (for details see Bellerby et al., 2007). The concomitant build-up of organic material, reflected by increasing Chl*a* concentrations showed also no treatment effect, although at the peak of the bloom total and diatom associated Chl*a* concentrations were seemingly higher in the 2x and 3x compared to the 1x CO_2 mesocosms. The build-up of particulate organic matter (POC, PON, POP), however, appeared slightly higher in the 3x compared to the 2x and 1x CO_2 mesocosms. The steady increase

in dissolved organic material (DOC, DON, DOP) on the other hand, was again not significantly different between CO_2 treatments. Also the build-up of metazooplankton (>90 μm) biomass was not significantly different between treatments. In summary, the temporal development of nutrient uptake, build-up and decline of particulate organic matter and increase of dissolved organic matter during the experiment followed the same patterns in all mesocosms, irrespective of CO_2 condition (compare Engel et al., 2005). The similarity of nutrient uptake and corresponding organic matter build-up between treatments could be caused by phytoplankton nutrient utilization (nitrate and phosphate) and division rates which are insensitive to changes in seawater pCO_2. Indeed, although there is a critical CO_2 concentration for all phytoplankton species below which their growth decreases, in the CO_2 range of the present study (350–1050 μatm) division rates of diatoms, coccolithophores and cyanobacteria have been found to be rather constant (Burkhardt et al., 1999a; Rost et al., 2002; Langer et al., 2006; Barcelos e Ramos et al., 2007). Changes in phytoplankton C/N and C/P stoichiometry due to variations of seawater pCO_2 would then have to explained by changes in inorganic carbon utilization (see below).

Another interesting finding is that deep water ammonium concentrations towards the end of the experiment increased to lower values in the 3x than in the 2x and than in the 1x CO_2 mesocosms (corresponding surface layer values show the same trend and increased from day t_{12} onwards due to deep water mixing). This can be explained by differences in remineralization rates of organic nitrogen compounds at depth. Ammonium regeneration in sediments appears to be oxygen dependent with steadily decreasing rates at decreasing oxygen concentrations Chapelle (1995); Serpa et al. (2007). But what could be the mechanisms responsible for reduced deep water oxygen concentrations at elevated CO_2? Although standing stocks of dissolved and particulate organic carbon in the upper surface waters were quite similar in all mesocosms, significantly more dissolved inorganic carbon was utilized in the 3x than in the 2x and than in the 1x CO_2 mesocosms (for details see Riebesell et al. (2007) and Bellerby et al., 2007). This implies that considerably more organic carbon must have been lost into deep wa-

ters, about twice as much in the 3x compared to the 1x CO_2 mesocosms. The process operating could be enhanced TEP formation which has been shown to be higher at elevated CO_2 (Engel , 2002), leading to intensified particle coagulation and hence organic carbon export from the surface to depth. Intensified organic carbon sedimentation at higher CO_2 levels could have fueled organic carbon remineralization by heterotrophic bacteria, leading to stronger oxygen reduction at depth in the 3x than in the 2x and than in the 1x CO_2 mesocosms. If only half of the additional organic carbon exported in the 3x CO_2 mesocosms would have been remineralized in the lower 1.5 m of of the mesocosms, oxygen would have been considerably stronger depleted at depth in comparison to the 2x and 1x CO_2 mesocosms, by about 100 μmol kg^{-1} at the end of the experiment. This could explain reduced ammonia regeneration at elevated CO_2.

4.3 Element ratios of particulate and dissolved organic matter

While in the surface layer element ratios of particulate and dissolved organic matter reflect processes of production and removal, corresponding ratios in the deep water of the mesocosms are indicative for processes of accumulation and remineralization. Until day t_9 element ratios of particulate organic matter were close to corresponding Redfield ratios. As from then on inorganic phosphorus was depleted while nitrate and dissolved inorganic carbon could still be assimilated, POC/POP and PON/POP steadily increased. The same trend was found for dissolved organic matter, although due to relatively high standard deviations statistically not significant. Interestingly, however, DOC/DON was considerably lower than the Redfield ratio , indicating preferential loss of dissolved organic carbon compared to dissolved organic nitrogen in all mesocosms. This can be the result of TEP formation, favoring preferential DOC export from the surface waters to depth (compare Sect. 5.2). In this context it is also important to note that the loss of organic matter from the surface, defined as the difference between organic matter build-up and the inorganic counterparts drawn-down, seems to be a process in operation right from the start of the experiment (data not shown but compare Riebesell et al., 2007).

Balancing the processes of accumulation and remineralization at depth is difficult because of the problems associated with sediment trap sampling and the lack of dissolved organic matter data in deep waters. However, the scenario described above of 1) increased loss of organic carbon from surface waters to depth at elevated CO_2, resulting in 2) increased respiration of this organic carbon and hence increased oxygen consumption at depth, and hence in 3) reduced organic nitrogen remineralization (ammonium regeneration) is not at odds with the observed patterns in sedimentary organic matter ratios. Constant sedimentary POC/PON, for instance, could indicate increased organic carbon remineralization at elevated CO_2. Furthermore, increased sedimentary PON/POP in the 3x and 2x in comparison to the 1x CO_2 mesocosms could be the result of decreased PON remineralization.

4.4 The pelagic ocean in a high CO_2 world: indications from mesocosm studies

Bulk parameters of natural phytoplankton blooms, especially those representative for biomass such as POC, PON, POP, Chl*a*, but also DOC, DON and DOP appear to a great extent insensitive to changing CO_2 conditions (compare Engel et al., 2005). Also corresponding elemental ratios of these standing stocks appear largely unaffected by seawater pCO_2. However, in this study there were pronounced treatment differences in the calculated amount of organic carbon lost from upper surface waters, with higher values in the 3x compared to the 2x and 1x CO_2 mesocosms (compare Riebesell et al., 2007). This was fueled by significantly increased dissolved inorganic carbon (DIC) to inorganic nutrient (nitrate, phosphate) uptake ratios at elevated CO_2 (compare Bellerby et al., 2007). Hence, elemental ratios of organic matter exported from surface to depth must have been enriched in organic carbon compared to nitrogen and phosphorus under elevated CO_2 conditions. Furthermore, this "extra" organic carbon could have resulted in higher bacterial respiration and oxygen consumption at depth, reducing ammonium regeneration in the 3x compared to the 2x and to the 1x CO_2 mesocosms.

In summary, mesocosm studies have identified various processes in pelagic ecosystems potentially sensitive to increasing atmospheric CO_2 (for details see Riebesell

et al., 2007[1]): 1) higher inorganic carbon consumption in the euphotic zone, 2) higher export production, 3) reduced ammonium regeneration at depth, 4) increases in climate relevant trace gas production (Wingenter et al., 2007), 5) reduced $CaCO_3$ production by coccolithophores such as *Emiliania huxleyi* (Delille et al., 2005) and 6) diminished growth and survival rates of calcifying molluscs (Antia et al., 2007). All these processes are part of feedback mechanisms impacting CO_2 partitioning between atmosphere and ocean. However, whether changes in these processes will dampen or enhance global climate change is still impossible to forecast.

Acknowledgements. We greatfully acknowledge the staff of the Espegrend Marine Biological Station, University Bergen, in particular T. Sørlie and A. Aadnesen, and the Bergen Marine Research infrastructure (RI) for helping organize and set up the mesocosm experiment. We also thank J. Barcelos e Ramos for processing the salinity data, and H.-P. Grossart, M. Vogt and J. Williams for helpful comments on the manuscript.

References

Antia, A., Suffrian, K., Holste, L., Müller, M. N., Nejstgaard, J. C., Simonelli, P., Carotenuto, Y., and Putzeys, S.: Dissolution of coccolithophorid calcite by microzooplankton and copepod grazing, Biogeosciences Discuss., accepted, 2007. 4553, 4558

Barcelos e Ramos, J., Biswas, H., Schulz, K. G., LaRoche, J., and Riebesell, U.: Effect of rising atmospheric carbon dioxide on the marine nitrogen fixer *Trichodesmium*, Glob. Biogeochem. Cycles, 21, doi:10.1029/2006GB002898, 2007. 4550

Bellerby, R. G. J., Schulz, K. G., Riebesell, U., Neill, C., Nondal, G., Johannessen, T., and Brown, K. R.: Marine ecosystem community carbon and nutrient uptake stoichiometry under varying ocean acidification during the PeECE III experiment, accepted, Biogeosciences Discuss., 2007. 4549, 4550, 4552, 4558

[1]Riebesell, U., Bellerby, R. G. J., Grossart, H.-P., and Thingstad, T. F.: Mesocosm CO_2 perturbation studies: from organism to community level, Biogeosciences Discuss., in preparation, 2007.

Burkhardt, S. and Riebesell, U.: CO_2 availability affects elemental composition (C:N:P) of the marine diatom *Sceletonema costatum*, Mar. Ecol. Prog. Ser., 155, 67–76, 1997. 4541

Burkhardt, S., Riebesell, U., and Zondervan, I.: Effects of growth rate, CO_2 concentration, and cell size on the stable carbon isotope fractionation in marine phytoplankton, Geochim. Cosmochim. Acta, 63, 3729–3741, 1999a. 4550

Burkhardt, S., Zondervan, I., and Riebesell, U.: Effect of CO_2 concentration on the C:N:P ratio in marine phytoplankton: A species comparision, Limnol. Oceanogr., 44, 683–690, 1999b. 4541

Caldeira, K. and Wicket, M. E.: Anthropogenic carbon and ocean pH, Nature, 425, p. 365, 2003. 4541

Carotenuto, Y., Putzeys, S., Simonelli, P., Paulino, A., Meyerhöfer, M., Suffrian, K., Antia, A., and Nejstgaard, J. C.: Feeding and reproduction of the copepod Calanus finmarchicus in nutrient-induced phytoplankton blooms under different CO_2 regimes: the Pelagic Ecosystem CO_2 Enrichment III (PeECE III) Mesocosm Experiment, Biogeosciences Discuss., 4, 3913–3936, 2007, http://www.biogeosciences-discuss.net/4/3913/2007/. 4558

Chapelle, A.: A preliminary model of nutrient cycling in sediments of a Mediterranean lagoon, Ecol. Mod., 80, 131–147, 1995. 4550

Delille, B., Harlay, J., Zondervan, I., Jacquet, S., Chou, L., Wollast, R., Bellerby, R. G. J., Frankignoulle, M., Borges, A. V., Riebesell, U., and Gattuso, J.-P.: Response of primary production and calcification to changes of pCO_2 during experimental blooms of the coccolithophorid *Emiliania huxleyi*, Glob. Biogeochem. Cycl., 19, doi:10.1029/2004GB002318, 2005. 4553

Egge, J. K., Thingstad, T. F., Engel, A., and Riebesell, U.: Primary production during nutrient-induced blooms at elevated CO_2 concentrations, Biogeosciences Discuss.,4, 4385–4410, 2007. 4558

Engel, A.: Direct relationship between CO_2 uptake and transparent exopolymer particles production in natural phytoplankton, J. Plankt. Res., 24, 49–53, 2002. 4541, 4551

Engel, A., Thoms, S., Riebesell, U., Rochelle-Newall, E., and Zondervan, I.: Polysaccharide aggregation as a potential sink of marine dissolved organic carbon, Nature, 428, 929–932, 2004. 4541

Engel, A., Zondervan, I., Aerts, K., Beaufort, L., Benthien, A., Chou, L., Delille, B., Gattuso, J.-P., Harlay, J., Heemann, C., Hoffmann, L., Jacquet, S., Nejstgaard, J., Pizay, M. D., Rochelle-

Newall, E., Schneider, U., Terbrueggen, A., and Riebesell, U.: Testing the direct effect of CO_2 concentration on a bloom of the coccolithophorid *Emiliania huxleyi* in mesocosm experiments, Limnol. Oceanogr., 50, 493–507, 2005. 4542, 4545, 4550, 4552

Gattuso, J.-P., Frankignoulle, M., Bourge, I., Romaine, S., and Buddemeier, R. W.: Effect of calcium carbonate saturation of seawater on coral calcification, Global Planet. Change, 18, 37–46, 1998. 4541

Hansen, H. P. and Koroleff, F.: Determination of nutrients, in: Methods of seawater analysis, 3. Edition, edited by: Grasshoff, K., Kremling, K., and Ehrhardt, M., 159–228, Wiley VCH, Weinheim, 1999. 4544, 4545

Holmes, R. M., Aminot, A., Kérouel, R., Hooker, B. A., and Peterson, B. J.: A simple and precise method for measuring ammonium in marine and freshwater ecosystems, Can. J. Fish. Aquat. Sci., 56, 1801–1808, 1999. 4544

IPCC: Climate Change 2001: The Scientific Basis. Contribution of Working Group I to the Third Assessment Report of the Intergovernmental Panel on Climate Change, edited by: Houghton, J. T., Ding, Y., Griggs, D. J., Nougher, M., van der Linden, P. J., Dai, X., Maskell, K. and Johnson, C. A., Cambridge University Press, Cambridge, United Kindom and New York, NY, USA, 2001. 4540, 4542

IPCC: Climate Change 2007: The Physical Science Basis. Contribution of Working Group I to the Fourth Assessment Report of the Intergovernmental Panel on Climate Change, edited by: Solomon, S., Qin, D., Manning, M., Chen, Z., Marquis, M., Averyt, K. B., Tignor, M., and Miller, H. L., Cambridge University Press, Cambridge, United Kindom and New York, NY, USA, 2007. 4540

Kleypas, J. A., Buddemeier, R. W., Archer, D., Gattuso, J.-P., Langdon, C., and Opdyke, B. N.: Geochemical consequences of increased atmospheric carbon dioxide on coral reefs, Science, 284, 118–120, 1999. 4541

Langer, G., Geisen, M., Baumann, K. H., Kläs, J., Riebesell, U., Thoms, S., and Young, J. R.: Species-specific responses of calcifying algae to changing seawater carbonate chemistry, Geochem. Geophys. Geosystems, 7, doi:10.1029/2005GC001227, 2006. 4541, 4550

Mackey, M. D., Mackey, D. J., Higgins, H. W., and Wright, S. W.: CHEMTAX – a program for estimating class abundances from chemical markers: application to HPLC measurements of phytoplankton, Mar. Ecol. Progr. Ser., 144, 265–283, 1996. 4544

Orr, J. C. Fabry, V. J., Aumont, O., Bopp, L., Doney, S. C., Feely, R. A., Gnanadesikan, A., Gruber, N., Ishida, A., Joos, F., Key, R. M., Lindsay, K., Maier-Reimer, E., Matear, R., Mon-

fray, P., Mouchet, A., Najjar, R. G., Plattner, G. K., Rodgers, K. B., Sabine, C. L., Sarmiento, J. L., Schlitzer, R., Slater, R. D., Totterdell, I. J., Weirig, M. F., Yamanaka, Y., and Yool, A.: Anthropogenic ocean acidification over the twenty-first century and its impact on calcifying organisms, Nature, 437, 681–686, 2005. 4541

Qian, J. and Mopper, K.: Automated High-Performance, High-Temperature Combustion Total Organic Carbon Analyzer, Anal. Chem., 68, 3090–3097, 1996. 4545

Riebesell, U.: Effects of CO_2 Enrichment on Marine Phytoplankton, J. Oceanogr., 60, 719–729, 2005. 4541

Riebesell, U., Zondervan, I., Rost, B., Tortell, P. D., Zeebe, R. E., and Morel, F. M. M.: Reduced calcification of marine plankton in response to increased atmosphe ric CO_2, Nature, 407, 364–367, 2000. 4541

Riebesell, U., Schulz, K. G., Bellerby, R. G. J., Botros, M., Fritsche, P., Meyerhöfer, N., Neill, C., G., N., Oschlies, A., Wohlers, J., and Zöllner, E.: Enhanced biological carbon consumption in a high CO_2 ocean, Nature, 450, 545–548, doi: 10.1038/nature06267, 2007. 4550, 4551, 4552

Rost, B., Zondervan, I., and Riebesell, U.: Light-dependent carbon isotope fractionation in the coccolithophorid *Emiliania huxleyi*, Limnol. Oceanogr., 47, 120–128, 2002. 4550

Russel, A. D., Hönisch, B., Spero, H. J., and Lea, D. W.: Effects of seawater carbonate ion concentration and temperature on shell U, Mg, and Sr in cultured planktonic foraminifera, Geochim. Cosmochim. Acta, 68, 4347–4361, 2004. 4541

Serpa, D., Falcão, M., Duarte, P., Cancela da Fonseca, L., and Vale, C.: Evaluation of ammonium and phosphate release from intertidal and subtidal sediments of a shallow coastal lagoon (Ria Formosa – Portugal): a modelling approach, Biogeochem., 82, 291–304, 2007. 4550

Sinha, V., Williams, J., Meyerhöfer, M., Riebesell, U., Paulino, A. I., and Larsen, A.: Air-sea fluxes of methanol, acetone, acetaldehyde, isoprene and DMS from a Norwegian fjord following a phytoplankton bloom in a mesocosm experiment, Atmos. Chem. Phys., 7, 739–755, 2007, http://www.atmos-chem-phys.net/7/739/2007/. 4558

Vogt, M., Steinke, M., Turner, S., Paulino, A., Meyerhöfer, M., Riebesell, U., Le Quére, C., and Liss, P.: Dynamics of dimethylsulphoniopropionate and dimethylsulfide under different CO_2 concentrations during a mesocosm experiment, Biogeosciences ,4(5), 3673–3699, 2007a. 4558

Wingenter, O. W., Haase, K. B., Zeigler, M., Blake, D. R., Sherwood Rowland, F. S., Sive, B. C., Paulino, A., Thyrhaug, R., Larsen, A., Schulz, K., Meyerhöfer, M., and Riebesell, U.: Unexpected consequences of increasing CO_2 and ocean acidity on marine production of DMS and CH_2CII: Potential climate impacts, Geophys. Res. Lett., 34, doi:10.1029/2006GL028139, 2007. 4553, 4558

Table 1. Measured parameters.

Parameter	Method	Reference
Temperature	CTD†	This article
Salinity	CTD†	This article
Alkalinity	Potentiometric Titration	Bellerby et al. (2007)
DIC	Coulometry	Bellerby et al. (2007)
$\delta^{13}C_{DIC}$	Mass spectrometry	U. Ninnemann et al.
pCO_2	Infrared analyzer Li-Cor 6262	Bellerby et al. (2007)
Nutrients	Autoanalyzer†	This article
Trace metals	Voltammetry	Breitbarth et al.(2007)[1]
Phytoplankton cell counts	Microscopy	V. Martin, unpubl. data
Phytoplankton and bacteria cell counts	Flowcytometry	Paulino et al.(2007)[2]
Pigments	HPLC†	This article
TPC, POC, PON	Elemental Analyzer†	This article
POP	Colorimetry†	This article
PIC	TPC-POC	This article
DOC, DON	HTCO†	This article
DOP	Colorimetry†	This article
TEP	Colorimetry	J. Wohlers unpl. data
Mono-, Polysaccharides	Colorimetry	J. Wohlers unpubl. data
Phosphorus uptake/affinity	$^{33}PO_4^{3-}$	Tanaka et al.(2007)[3]
Primary Production	^{14}C incubation, oxygen L/D method	Egge et al. (2007)
C-fluxes	^{13}C labelling of biomarkers	J. Middelburg unpl. data
Micro and mesozooplankton	Microscopy	Antia et al. (2007), Suffrian et al.(2007)[4]
Copepod eggs and fecal pellets	Microscopy	Carotenuto et al. (2007)
Bacterial diversity/production	DGGE	Allgaier et al.(2007)[5]
Glucose, APA affinity/turnover	^{14}C labelling / Fluorometry	Tanaka et al.(2007)[3]
Viral density/diversity	Flowcytometry / DGGE,PFGE	Larsen et al.(2007)[6]
VOC in headspace	PTR-MS	Sinha et al. (2007)
Organohalogens in headspace	GC-MS	–
DMS, DMSP, DMSP lyase	GC	Vogt et al. (2007a); Vogt et al.(2007b)[7]
Organic sulfur compounds, halocarbons, hydrocarbons, alkyl nitrates	GC-FID-ECD-MS	Wingenter et al. (2007)
Remineralization	Bottle incubations	NERI, Roskilde

Table 1. Continued.

† for details see Materials and Methods section of this article.

[1] Breitbarth, E., Bellerby, R. J., Neill, C., Ardelan, M. V., Meyerhöfer, M., Zöllner, E., Croot, P. L., and Riebesell, U.: Ocean acidification increases bioavailability of iron, Science (in review), 2007.

[2] Paulino, A., Egge, J., and Larsen, A.: Dynamics of small and intermediate sized osmotrophs at different CO_2 levels, Biogeosciences Discuss., in preparation, 2007.

[3] Tanaka, T., Thingstad, T. F., Allgaier, M., Egge, J. K., Grossart, H.-P., Larsen, A., Løvdal, T., Meyeröfer, M., Riebesell, U., Schulz, K. G., Wohlers, J., and Zöllner, E.: Implications of reduced phosphate availability for phytoplankton and bacteria at higher pCO_2 levels in a mesocosm study, Biogeosciences Discuss., in preparation, 2007.

[4] Suffrian, K., Simonelli, P., Antia, A., Putzeys, S., Carotenuto, Y., and Nejstgaard, J. C.: Phytoplankton-zooplankton grazing and growth interactions during the PeECE III mesocosm study 2005, Biogeosciences Discuss., in preparation, 2007.

[5] Allgaier, M., Riebesell, U., and Grossart, H.-P.: Coupling of heterotrophic bacteria to phytoplankton bloom development at different pCO_2 levels: a mesocosm study, Biogeosciences Discuss., in preparation, 2007.

[6] Larsen, J. B., Larsen, A., Thyrhaug, R., Bratbak, G., and Sandaa, R.-A.: Marine viral populations at elevated nutrient and pCO_2 levels, Biogeosciences Discuss., in preparation, 2007.

[7] Vogt, M., Turner, S., Yassaa, N., Steinke, M., Williams, J., and Liss, P.: Laboratory inter-comparison of dissolved dimethyl sulfide (DMS) measurements using purge-and-trap and solid-phase microextraction techniques during a mesocosm experiment, submitted to Marine Chemistry, 2007b.

BGD
4, 4539–4570, 2007

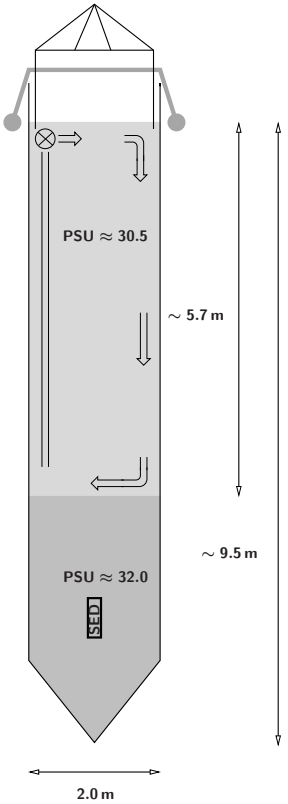

Fig. 1. Mesocosm design and setup. PSU denotes Salinity and SED the sediment trap. See text for details.

BGD
4, 4539–4570, 2007

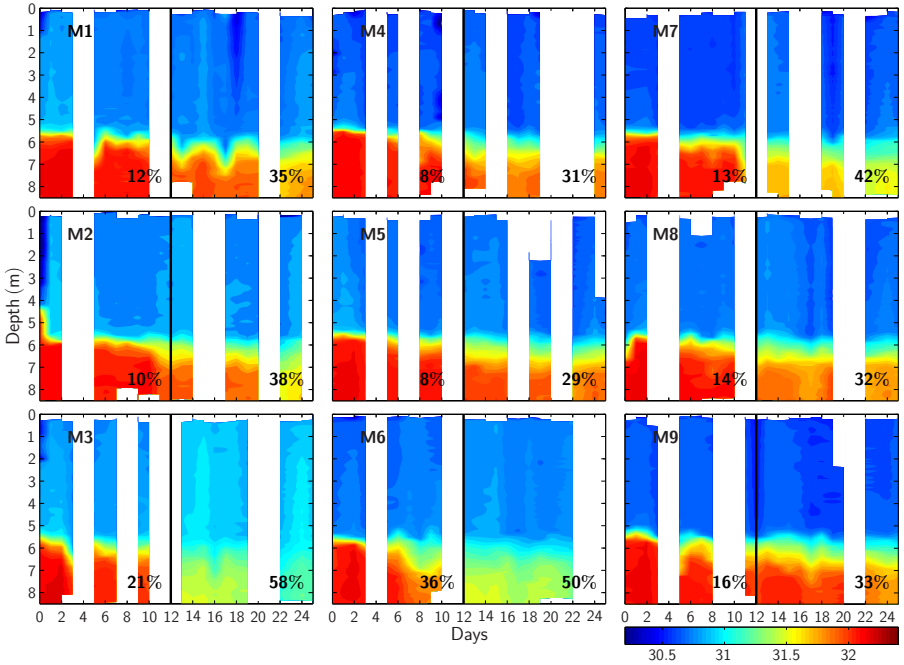

Fig. 2. Temporal changes in the vertical distribution of salinity within each mesocosm during the experiment. The black vertical lines mark the "storm event" around day 12. The loss of deep water into the upper 5.7 m by mixing was calculated from a simple mass balance. Numbers prior to day 12 denote the loss until day 10 while numbers after day 12 denote the loss until the end of the experiment.

BGD
4, 4539–4570, 2007

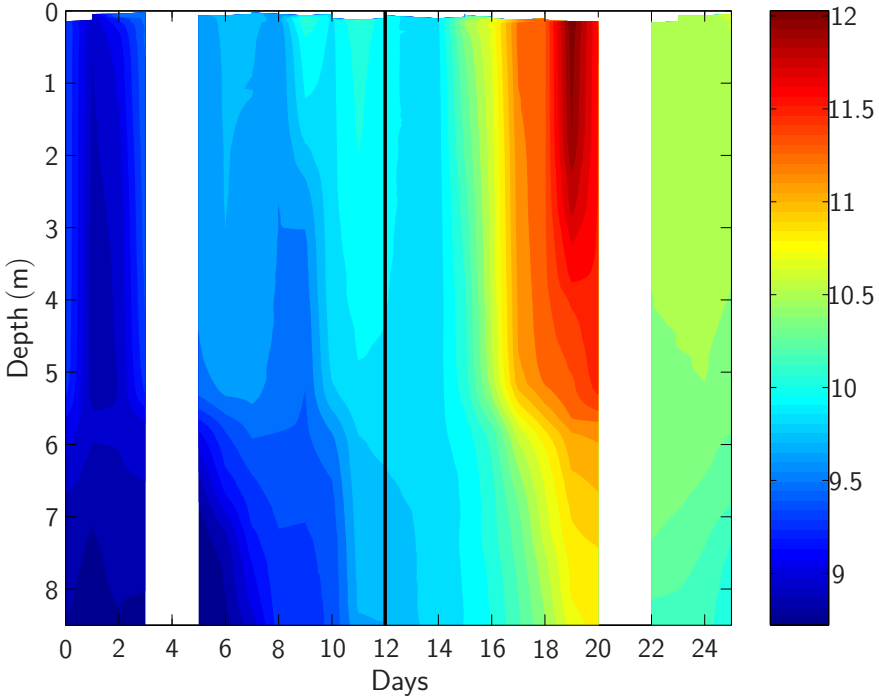

Fig. 3. Temporal changes in the vertical temperature distribution averaged along all nine mesocosms. Standard deviation between mesocosms was generally less than 0.1°C. The vertical black line marks the "storm event" around day 12.

BGD
4, 4539–4570, 2007

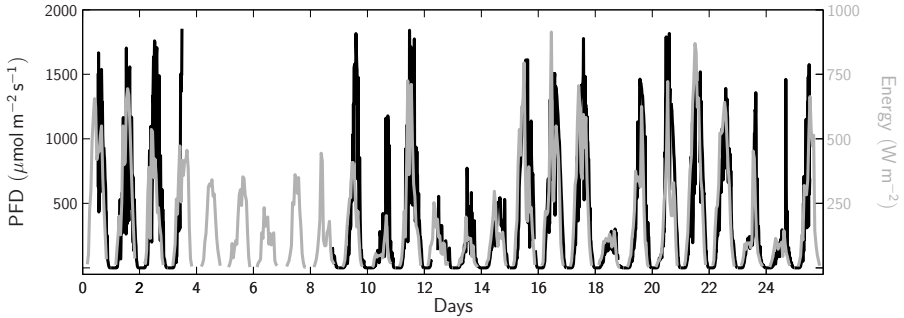

Fig. 4. Photon flux density (PFD) of incident photosynthetic active radiation between 400 and 700 nm (PAR) as measured on the raft (black line) and total amount of energy received as measured by the Geophysical Institute of the University of Bergen (grey line). See results section for details on PFDs within the mesocosms headspace and mixed surface water.

BGD
4, 4539–4570, 2007

EGU

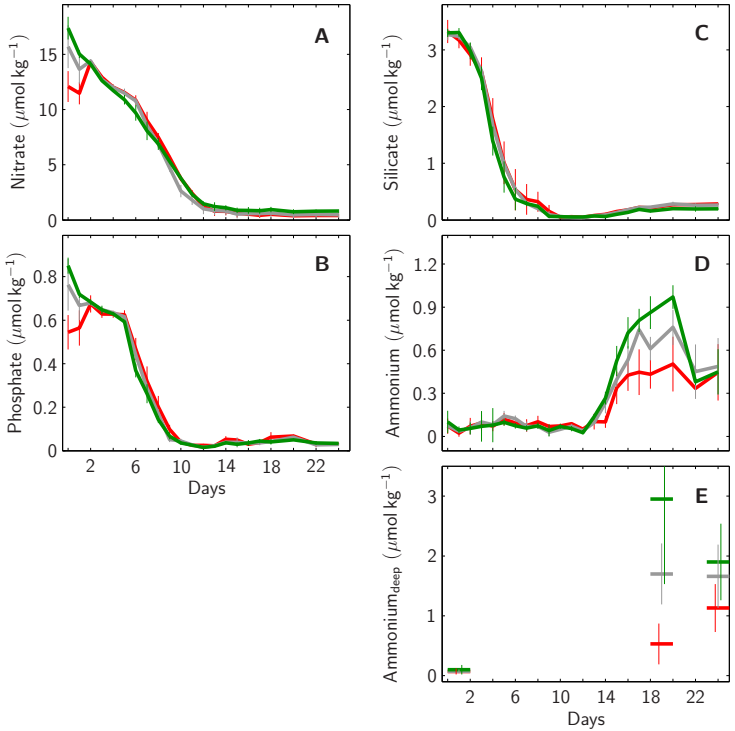

Fig. 5. Temporal development of major nutrient concentrations within the mesocosms' upper mixed layer. Green, grey and red lines illustrate average concentrations of **(A)** nitrate, **(B)** phosphate, **(C)** silicate and **(D)** ammonium within the 1x, 2x and 3x CO_2 mesocosms, respectively. **(E)** Ammonium concentrations measured in deep waters at the beginning of the experiment (t_0) and selected days towards the end (t_{20} and t_{25}). Vertical lines denote standard deviations within each CO_2 treatment (1x, 2x, 3x CO_2).

BGD
4, 4539–4570, 2007

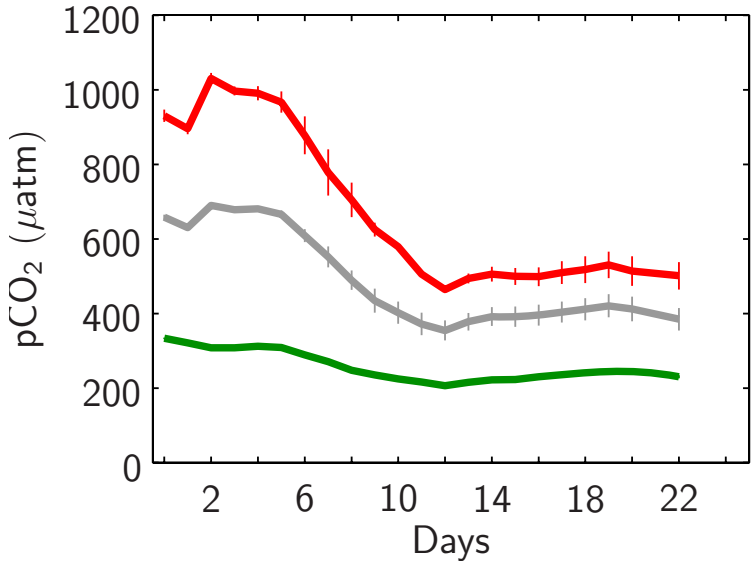

Fig. 6. Temporal development of CO_2 partial pressures (pCO_2) within the mesocosms' upper mixed layer. Style and color-coding follow that of Fig. 5.

BGD
4, 4539–4570, 2007

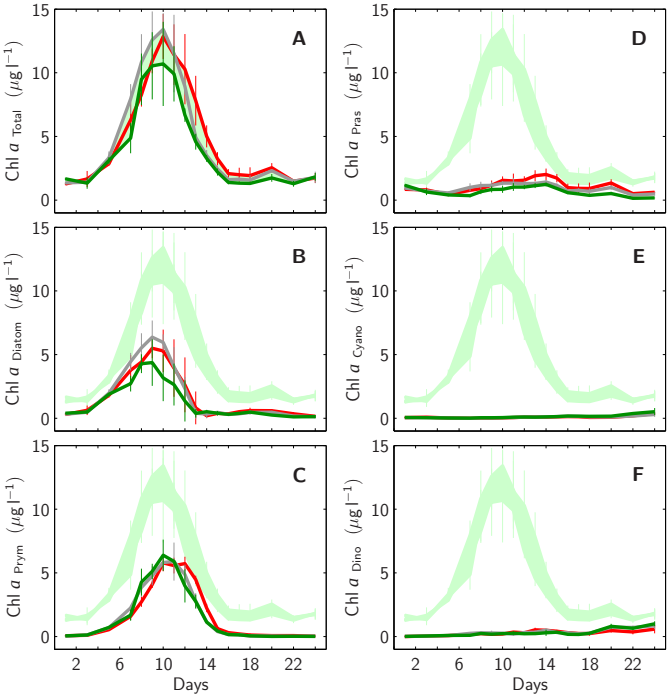

Fig. 7. Temporal development of Chl*a* concentrations within the mesocosms' upper mixed layer. Total Chl*a* concentrations **(A)** were measured by HPLC, while individual Chl*a* contributions by diatoms **(B)**, prymnesiophytes **(C)**, prasinophytes **(D)**, cyanobacteria **(E)** and dinoflagellates **(F)** have been calculated using the CHEMTAX algorithm (see methods for details). Shaded light green area depicts the temporal and spatial range of total Chl*a* within all mesocosms. Style and color-coding follow that of Fig. 5.

BGD
4, 4539–4570, 2007

EGU

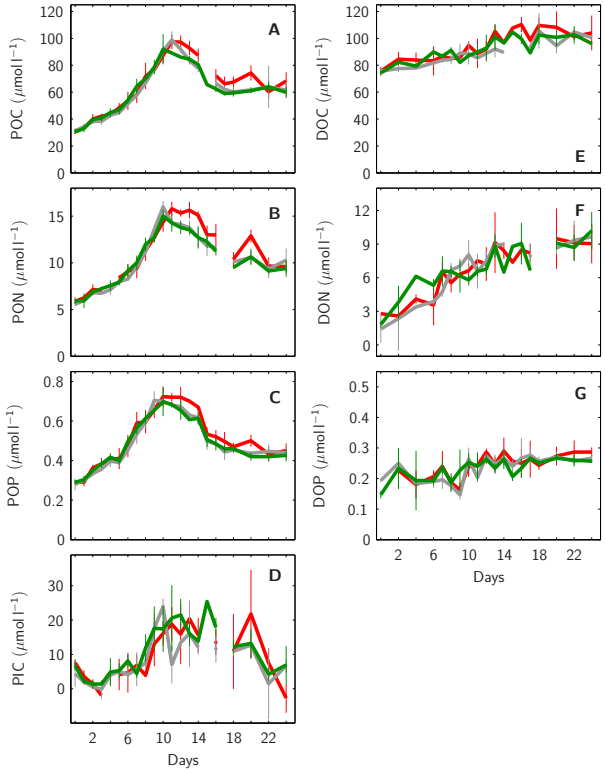

Fig. 8. Temporal development of organic matter within the mesocosms' upper mixed layer. Standing stocks of particulate organic matter POC **(A)**, PON **(B)**, POP **(C)** and PIC **(D)** are shown in comparison to those of dissolved organic matter DOC **(E)**, DON **(F)** and DOP **(G)**. Style and color-coding follow that of Fig. 5.

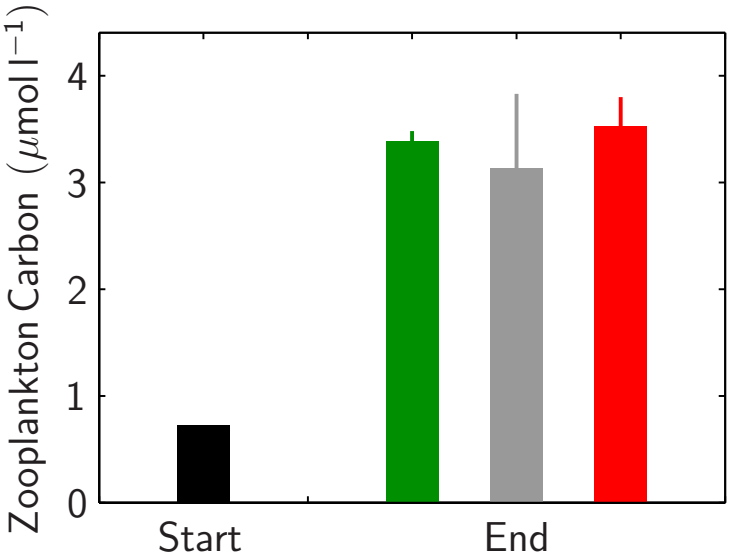

Fig. 9. Average metazooplankton (>90 μm) organic carbon at the start (black) and at the end of the experiment in the 1x CO_2 (green), 2x CO_2 (grey) and 3x CO_2(red) mesocosms. Vertical lines denote standard deviations.

BGD
4, 4539–4570, 2007

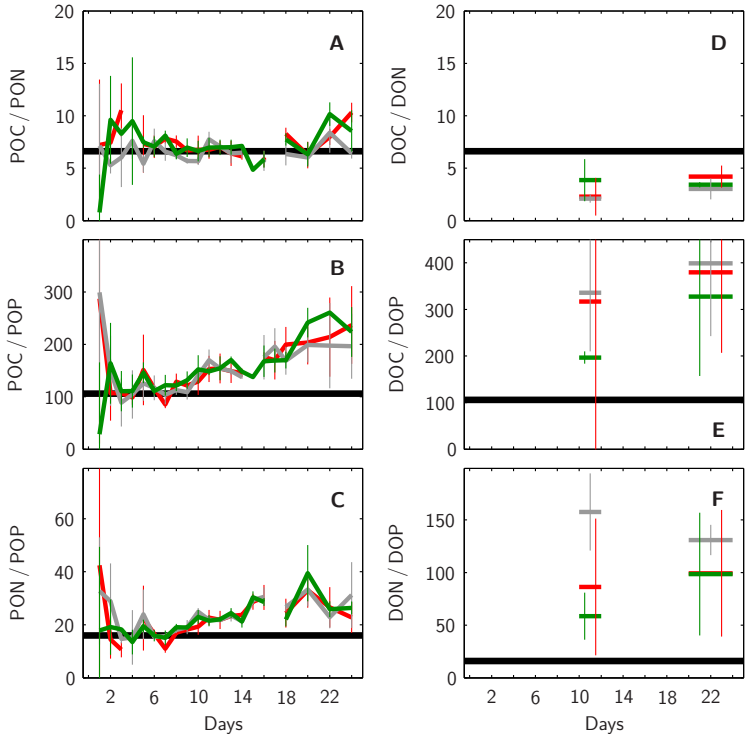

Fig. 10. Temporal development in element ratios of particulate organic and dissolved organic matter produced in the mesocosms' upper surface waters. Ratios shown are POC/PON **(A)**, POC/POP **(B)**, PON/POP **(C)**, DOC/DON **(D)**, DOC/DOP **(E)**, and DON/DOP **(F)**. Ratios of particulate organic matter were determined from organic matter build-up starting from t_0–t_1 averages in each mesocosm (A, B and C). Ratios of dissolved organic matter were estimated from corresponding build-up until the peak and end of the bloom, t_{11}–t_{12} and t_{20}–t_{24}, respectively, starting from t_0–t_4 averages (D, E and F). Style and color-coding follow that of Fig. 5. Black horizontal lines denote respective Redfield ratios.

BGD
4, 4539–4570, 2007

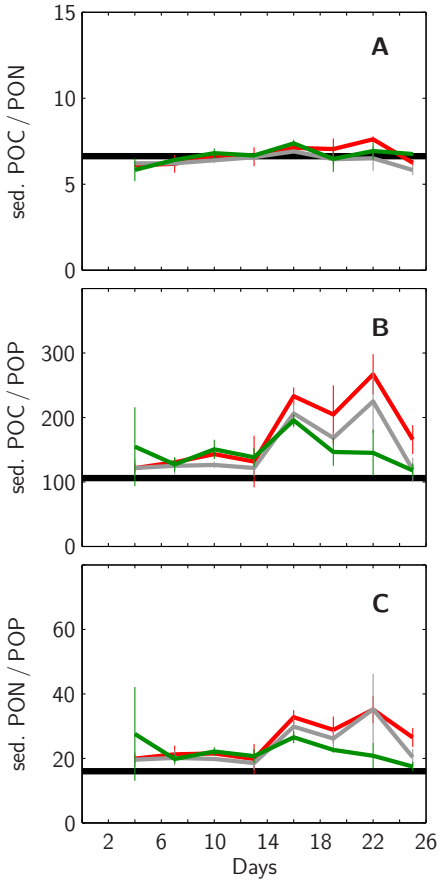

Fig. 11. Temporal development in elemental ratios of particulate organic matter sampled by sediment traps. Shown are sedimentary ratios of POC/PON **(A)**, POC/POP **(B)**, and PON/POP **(C)**. Style and color-coding follow that of Fig. 5. Black horizontal lines denote respective Redfield ratios.

BGD
4, 4539–4570, 2007